

# ICRF Plasma Production with Hydrogen Minority Heating in Uragan-2M and Large Helical Device<sup>\*)</sup>

Yurii V. KOVTUN<sup>1)</sup>, Vladimir E. MOISEENKO<sup>1,2,3)</sup>, Shuji KAMIO<sup>4)</sup>, Hiroshi KASAHARA<sup>5)</sup>, Tetsuo SEKI<sup>5)</sup>, Kenji SAITO<sup>5)</sup>, Ryosuke SEKI<sup>5)</sup>, Alexei V. LOZIN<sup>1)</sup>, Rostislav O. PAVLICHENKO<sup>1)</sup>, Anatolii N. SHAPOVAL<sup>1)</sup>, Igor E. GARKUSHA<sup>1,2)</sup>, Arturo ALONSO<sup>6)</sup>, Andreas DINKLAGE<sup>7)</sup>, Dirk HARTMANN<sup>7)</sup>, Yevgen O. KAZAKOV<sup>8)</sup>, Heinrich LAQUA<sup>7)</sup>, Josef ONGENA<sup>8)</sup>, Torsten STANGE<sup>7)</sup> and Tom WAUTERS<sup>9)</sup>

<sup>1)</sup>*Institute of Plasma Physics of the NSC KIPT, Kharkiv, Ukraine*

<sup>2)</sup>*V.N. Karazin Kharkiv National University, Kharkiv, Ukraine*

<sup>3)</sup>*Ångström Laboratory, Uppsala University, Uppsala, Sweden*

<sup>4)</sup>*University of California Irvine, Irvine, CA, United States of America*

<sup>5)</sup>*National Institute for Fusion Science, Toki, Japan*

<sup>6)</sup>*Laboratorio Nacional de Fusion, CIEMAT, Madrid, Spain*

<sup>7)</sup>*Max-Planck-Institut für Plasmaphysik, Greifswald, Germany*

<sup>8)</sup>*Laboratory for Plasma Physics, ERM/KMS, Brussels, Belgium*

<sup>9)</sup>*ITER Organization, St. Paul-lez-Durance, France*

(Received 7 January 2023 / Accepted 11 April 2023)

This report compares results ion-cyclotron range of frequencies (ICRF) plasma production at hydrogen minority regime in Uragan-2M (U-2M) and Large Helical Device (LHD). The condition of the presence of the fundamental harmonic ion cyclotron resonance zone for the hydrogen inside the plasma column should be fulfilled for this method. The scenario is successful at both machines and weakly sensitive to the variation of the hydrogen concentration in the H<sub>2</sub>+He gas mixture. It should be noted that at LHD the start up is slower than at U-2M. The comparison of plasma production in ICRF with hydrogen minority at U-2M and LHD indicate that this scenario can be scaled to larger stellarator devices. The experiments made are the base for the proposal for usage this scenario for plasma production in ICRF at Wendelstein 7-X at magnetic field reduced to 1.7 T.

© 2023 The Japan Society of Plasma Science and Nuclear Fusion Research

Keywords: plasma production, ion cyclotron heating, stellarator, Uragan-2M, Large Helical Device, RF power

DOI: 10.1585/pfr.18.2402042

## 1. Introduction

The optimized superconducting stellarator device Wendelstein 7-X (W7-X) in Greifswald, Germany, is the first HELIAS machine that aims to demonstrate that power plant requirements can be achieved in a stellarator [1]. The W7-X has several heating systems: the electron-cyclotron resonance heating (ECRH) [2], the neutral beam injection (NBI) [3] and the ion-cyclotron resonance heating (ICRH) [4, 5]. The regular magnetic field of W7-X that fits to X2 ECRH is 2.5 T. The operation of W7-X at the magnetic field of 1.7 T is possible with usage of 3rd harmonic ECRH (X3-mode). The experiments at this magnetic field give an opportunity to investigate high  $\beta$  plasma and more magnetic configurations. The experimental [6] studies and the theory [7] show a need to create a target plasma for X3-mode ECRH. The initial plasma can be created by radio-frequency ICRF system in the ion-cyclotron

resonance range on W7-X [4, 5], possibly with an intermediate heating step by NBI.

The motivation of this study is to provide plasma creation in conditions at which ECRH startup is not possible, and in this way to widen the operational frame of helical machines. The experiments on stellarator Uragan-2M (U-2M) support the W7-X experimental program on ICRF. Based on plasma production experiments in U-2M, a scenario had been proposed for ICRF plasma production at the hydrogen minority regime [8–11]. However, the U-2M is notably smaller than Large Helical Device (LHD) and W7-X. Moreover, the magnetic field in U-2M is an order of magnitude lower. The initial experiments at LHD [12] device confirmed that the minority scenario is possible in large machines. This paper presents new studies on the ICRF plasma production at hydrogen minority regime in U-2M and LHD in comparison with previous ones.

author's e-mail: kovtun41@gmail.com

<sup>\*)</sup> This article is based on the presentation at the 31st International Toki Conference on Plasma and Fusion Research (ITC31).

## 2. Experimental Devices

### 2.1 Uragan-2M

The U-2M device at Kharkiv, Ukraine, is a medium-size stellarator of torsatron type [8, 13, 14]. The magnetic system is water cooled and consists of  $l = 2$  helical coils with four periods ( $m = 4$ ) in the toroidal direction. U-2M is equipped with 16 coils producing a toroidal field. The magnetic configuration parameters can be changed varying the parameter  $K_\phi = B_{th}/(B_{tt} + B_{th})$  where  $B_{tt}$  and  $B_{th}$  are the toroidal fields at the geometrical axis of the torus produced by the toroidal and helical coils, respectively. The magnetic field power system makes it possible to operate at  $B_0 < 0.6$  T where  $B_0 = B_{tt} + B_{th}$ . The U-2M stellarator use only RF methods to produce and heat plasma [8–11, 15–17]. For this purpose, two identical pulsed RF systems the ‘Kaskad-1’ (K-1) and ‘Kaskad-2’ (K-2) [8] are used. The U-2M has several antennas: the frame antenna (FA) [15], three-half-turn antenna (THTA) [16] and two-strap antenna (TSA) [8, 17]. The TSA antenna is mimicking the W7-X ICRF antenna [4, 5] and the main difference is that it is smaller. The antenna consists of two parallel poloidal straps oriented perpendicular to the toroidal axis [8, 17]. The TSA antenna used for plasma production at hydrogen minority regime [8–11]. The main characteristics of the U-2M are shown in Table 1.

### 2.2 Large Helical Device

The LHD is a large-scale heliotron-type superconducting device at Toki, Japan [18]. The poloidal and toroidal period field period numbers are  $l/m = 2/10$ . The LHD has several heating systems: the ECRH, the NBI and the ICRH [19]. The ion cyclotron range of frequencies (ICRF) heating system in the LHD is used with a fixed frequency of 38.47 MHz [20] and has maximum output power 3 MW [21]. The two types of antennas are used on the LHD: a Hand-Shake form antennas (HAS) [22] and a Field-Aligned-Impedance Transforming antennas (FAIT) [23]. The antennas occupy the upper (U) and lower (L) ports of the LHD vacuum chamber. The strap elements of both antennas are oriented perpendicular to the magnetic field and are shielded by the Faraday screens. The main characteristics of the LHD are shown in Table 1.

## 3. Hydrogen Minority Scenario

The main requirement for this scenario is the pres-

Table 1 Devices characteristics.

	U-2M	LHD
Major radius, $R$ (m)	1.7	3.9
Minor radius, $r$ (m)	0.34	0.6
Plasma volume, $V_p$ (m <sup>3</sup> )	~ 1.6	~ 30
Magnetic field, $B$ (T)	< 0.6	3
Total heating power, (MW)	< 0.4	36
Plasma heating tools	ICRF	ECRH, NBI, ICRF

ence of minority hydrogen ions in the plasma. The ion cyclotron resonance zone for the hydrogen fundamental harmonic should be present inside the plasma column [8, 9]. The main mechanism of plasma formation is the ionization of neutral atoms (molecules) by electron impact. At low plasma densities, the heating of electrons is due to slow wave (SW) excitation by the antenna and its absorption by plasma. At higher plasma densities, a fast wave (FW) propagates. In the layer where the Alfvén resonance condition is fulfilled, FW is converted to SW. SW propagates toward the lower hybrid resonance (LHR) layer, where SW is completely absorbed [8].

This scenario was developed at U-2M [8, 9] and was qualified for ICRF plasma generation in the LHD [12].

## 4. Experimental Results

### 4.1 Experimental results at U-2M

The experimental results presented here were obtained in the experimental campaigns of years 2019–2021 on U-2M [8–11]. The TSA antenna was used to production the plasma [8, 17]. The RF frequency was equal to the fundamental hydrogen ion cyclotron harmonic  $\omega_{RF} \approx \omega_{ci} (H^+) \approx 2\omega_{ci} (He^{2+}) \approx 4\omega_{ci} (He^+)$  in these experiments. The cyclotron zone was located inside the plasma column. Gas mixtures were prepared before the experiments in the gas mixture system [24]. The percentage composition of the mixture in the U-2M vacuum chamber was measured by a mass spectrometer.

In the first experiments (experimental campaign Spring-2019 on U-2M), the plasma was production in a pure helium [8] at an initial pressure  $0.14 - 4 \times 10^{-2}$  Pa. A small concentration of hydrogen minority spontaneously entered the plasma, presumably due to the dissociation of water and hydrocarbons. Accordingly, the hydrogen concentration in the plasma was not controlled. At an injected RF power of ~100 kW production of plasma with a density  $(2 - 2.6) \times 10^{18} \text{ m}^{-3}$  was observed near the first harmonic of the hydrogen cyclotron frequency. Further experiments in the helium pressure range of  $0.145 - 1.6 \times 10^{-2}$  Pa have shown that at  $p < 3 \times 10^{-2}$  Pa the plasma density decreases significantly [9]. The shot by shot dependence of the average plasma density on the pressure of helium is shown in Fig. 1. The maximum average plasma density obtained in helium did not exceed a value of  $\approx 3 \times 10^{18} \text{ m}^{-3}$  in the range of pressures below ~0.1 Pa [9, 11]. A further increase in high-frequency power did not lead to a significant increase in the plasma density. As a result, the degree of plasma ionization was not high. Analogous results on production of plasma in helium ion cyclotron wall conditioning (ICWC) discharge were previously obtained on tokamak TEXTOR-94 [25] and stellarator W7-AS [26].

In the case of a controlled concentration of hydrogen minority in helium, a higher plasma density is achieved and the degree of gas ionization is significantly increased [9–11]. In the first experiments (experimental campaign

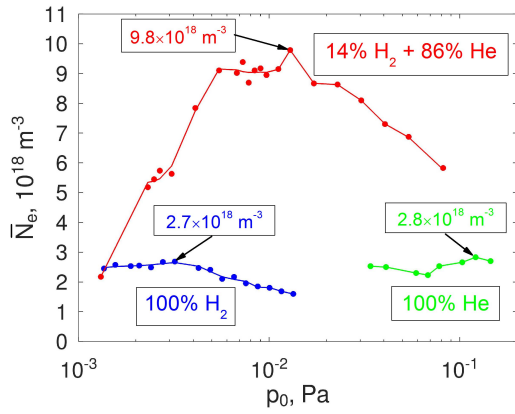


Fig. 1 Maximum average plasma density as a function of the pressure ( $U_a = 7$  kV,  $f = 4.9$  MHz) 14% $H_2$ +86%He,  $B_0 = 0.35$  T, 100% $H_2$ ,  $B_0 = 0.324$  T, 100%He,  $B_0 = 0.326$  T.

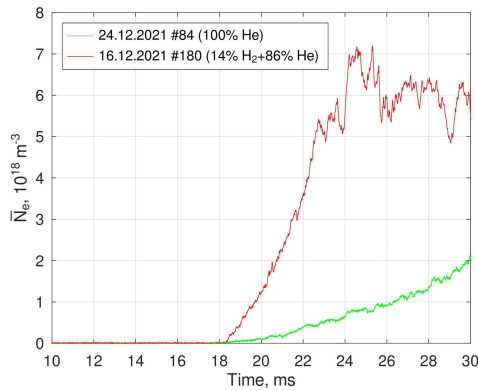


Fig. 2 Time evolutions of average plasma density for He and gas mixture 14% $H_2$ +86%He for initial pressure  $p_0 = 3.4 \times 10^{-2}$  Pa and  $U_a = 7$  kV. (for He  $B_0 = 0.325$  T,  $K_\phi = 0.325$ ,  $f = 4.96$  MHz; for 14% $H_2$ +86%He,  $B_0 = 0.32$  T,  $K_\phi = 0.34$ ,  $f = 4.9$  MHz).

Spring-2020 on U-2M) in the  $H_2$ +He mixture, the average plasma density was obtained  $\sim 2.6$  times higher than in pure helium at the initial pressure of the  $H_2$ +He mixture  $\sim 20$  times lower [9]. Consequent experiments (experimental campaigns Fall-2020 and Fall-2021 on U-2M) has focused on a more detailed investigation of plasma production in  $H_2$ +He mixture with controlled concentration of hydrogen minority [10,11]. Figure 1 shows a comparison of the average plasma density formed in the  $H_2$ +He gas mixture and in helium. At the same initial pressure  $\sim 3.5 \times 10^{-2}$  Pa, the plasma density is  $\sim 3.2$  times higher for the  $H_2$ +He mixture. The dynamics of the plasma density increase is also different for the  $H_2$ +He and He. Figure 2 shows the time evolution of the average plasma density at the same initial pressure for He and the  $H_2$ +He mixture. For RF discharges in helium, a smooth increase in the plasma density over a time of more than 12 ms is characteristic. At the same time, the achieved maximum density did not exceed the value of  $\approx 2.6 \times 10^{18} \text{ m}^{-3}$ . In the  $H_2$ +He mixture, the maximum density of  $\approx 7 \times 10^{18} \text{ m}^{-3}$  was reached in 6 ms. The

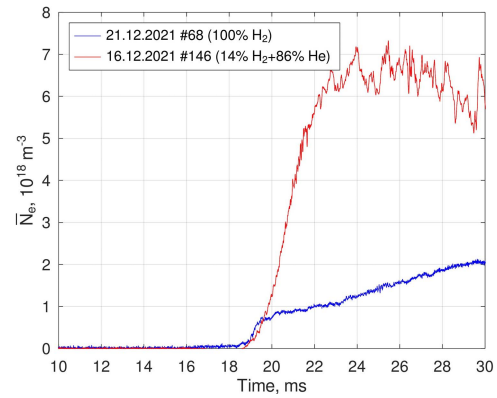


Fig. 3 Time evolutions of average plasma density for  $H_2$  and gas mixture 14% $H_2$ +86%He for initial pressure  $p_0 = 5 \times 10^{-3}$  Pa and  $U_a = 7$  kV. (for  $H_2$   $B_0 = 0.32$  T,  $K_\phi = 0.34$ ,  $f = 4.96$  MHz; for 14% $H_2$ +86%He,  $B_0 = 0.32$  T,  $K_\phi = 0.34$ ,  $f = 4.9$  MHz).

fluctuations in the plasma density are observed. For pure hydrogen, the dependence of plasma density on pressure is similar to that obtained in helium (see Fig. 1). In hydrogen and in helium, the maximum plasma density weakly varies less than  $\sim 2$  times in the experimental neutral gas pressure range. The maximum plasma density in hydrogen was lower than  $\approx 3 \times 10^{18} \text{ m}^{-3}$ . At an initial pressure of  $\sim 1.5 \times 10^{-2}$  Pa, the plasma density is higher by a factor of  $\sim 6.3$  for the  $H_2$ +He mixture (see Fig. 1). At formation of plasma (see Fig. 3) in hydrogen, there is a rapid increase in density to  $\approx 0.78 \times 10^{18} \text{ m}^{-3}$  in the initial period of 18 - 19.5 ms, followed by a smooth increase in plasma density to a maximum value of  $\approx 2.1 \times 10^{18} \text{ m}^{-3}$ . In a mixture of  $H_2$ +He increase of plasma density is observed to a maximum value of  $\approx 7 \times 10^{18} \text{ m}^{-3}$  for 6 ms and subsequent fluctuations in plasma density.

Studies of plasma production in  $H_2$ +He mixture showed [9–11] that the density of the produced plasma depends on the injected RF power, the hydrogen concentration in the mixture, and the initial pressure of the mixture. A simple estimate based on U-2M results indicates that to create a plasma with high density, RF power density at or above  $60 \text{ kW/m}^3$  is required. The optimal concentration is 14% hydrogen that provides plasma production of highest density. Increase or decrease of hydrogen concentration  $\approx 2$  times leads to decrease of plasma density in  $\sim 1.2$  times.

The temperature of electrons and plasma ions measured by optical spectral methods was not more than a few tens of eV. Accordingly, the created plasma had a noticeable density and low temperature. Note that in the experiments on producing plasma in  $H_2$ +He ICWC discharge mixture conducted in tokamaks were obtained significantly lower plasma densities up to  $\approx 5 \times 10^{17} \text{ m}^{-3}$  [27–30].

## 4.2 Experimental results at LHD

Experimental results were obtained in the 22th [12] and 23th experimental campaigns on LHD. The ICRF

plasma production scenario with minority hydrogen ions at LHD [12] was similar to that developed at U-2M [8, 9]. Accordingly, the ion cyclotron resonance zone for the hydrogen fundamental harmonic was inside the plasma column. The main differences between the experiments at LHD and at U-2M were the significantly higher magnetic field of 2.55 and 2.75 T in LHD, the larger plasma volume  $\sim 30 \text{ m}^3$ , the RF power up to 2 MW, and usage of two types of antennas, FAIT and HAS. An  $\text{H}_2 + \text{He}$  gas mixture with controlled hydrogen concentration was created in the LHD vacuum chamber by independently injecting  $\text{H}_2$  and He. The percentage composition of the mixture was measured by a quadrupole mass spectrometer.

In the first experiments on the LHD (22th experimental campaign on LHD), the plasma was produced in the  $\text{H}_2 + \text{He}$  mixture [12] at injected RF power up to 0.3 MW. The main limitation of these experiments was the low RF power to reduce the probability of arcing on the RF system elements. No dangerous voltage rise on the RF system elements and arcing was detected. Two regimes were realized: ICRH with pre-ionization by the ECRH and ICRH solely. In the first regime with pre-ionization the preliminary plasma was created by the ECRH discharge. Further on plasma decay after ECRH pulse, the ICRF power was injected. In the second regime, without pre-ionization, the plasma was produced only by ICRF discharge. In both regimes, the ICRF discharge maintained a plasma of low density and the antenna-plasma coupling is far from optimal. As a result, the ICRF discharge at a specific RF power density of  $\sim 7 \text{ kWm}^{-3}$  created a plasma with a density of  $\approx 9.5 \times 10^{17} \text{ m}^{-3}$  [12].

In subsequent experiments (23th experimental campaign on LHD), the injected RF power was significantly increased. To prevent undesirable events arising on the antenna (occurrence of arcs, RF breakdown on antenna elements) in case of no-load (low plasma density) RF power was introduced smoothly (see Figs. 4 and 5). Two regimes were also realized: ICRH with pre-ionization by the ECRH and the ICRH alone. As an illustration of the ICRH with pre-ionization by the ECRH of the regime with Fig. 4 shows the plasma parameters evolutions for one of the shots. In the first stage, a plasma of density  $\approx (8 - 9.3) \times 10^{18} \text{ m}^{-3}$  was produced and maintained only by an ECRH discharge with a power of  $\approx 1 \text{ MW}$ . The ECRH discharge produced a dense, highly ionized hot plasma. After the ECRH pulse, the plasma density increases slightly and after  $\approx 4.95 \text{ s}$  the plasma density begins to decrease. The intensity of the spectral lines H I, He I, and impurities C III, CIV, and O V increases due to recombination (see Fig. 4). In the second stage, RF power up to 1.75 MW was injected into the plasma with a density below  $\approx 1 \times 10^{17} \text{ m}^{-3}$  after 5.42 s. The plasma density increased to  $\approx 10 \times 10^{18} \text{ m}^{-3}$ . The intensity of the spectral lines also increased. Further, the RF power decreased to 1.25 MW. The plasma density also decreased to  $\approx 3 \times 10^{18} \text{ m}^{-3}$ . The temperature of the electrons in the ICRF discharge was low, as in the first ex-

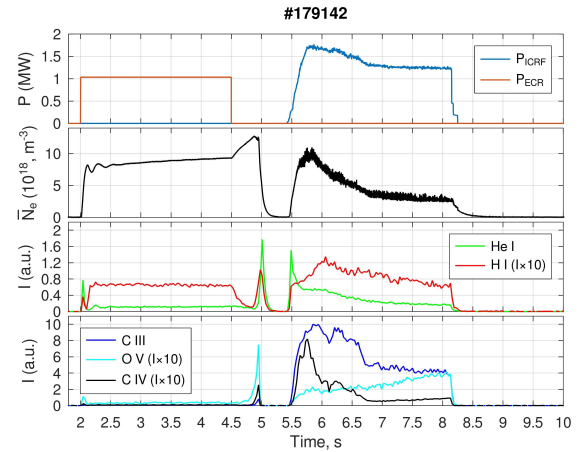


Fig. 4 Time evolutions of injection powers  $P_{\text{ICRF}}$  (total) and  $P_{\text{ECR}}$ , average electron density  $N_e$ , optical emission intensities of H I ( $\text{H}\alpha$  656.3 nm), He I (587.6 nm), C III (97.7 nm), O V (63 nm) and CIV (154.9 nm). The working gas content is 33%  $\text{H}_2$  + 67% He.  $B_0 = 2.75 \text{ T}$ .

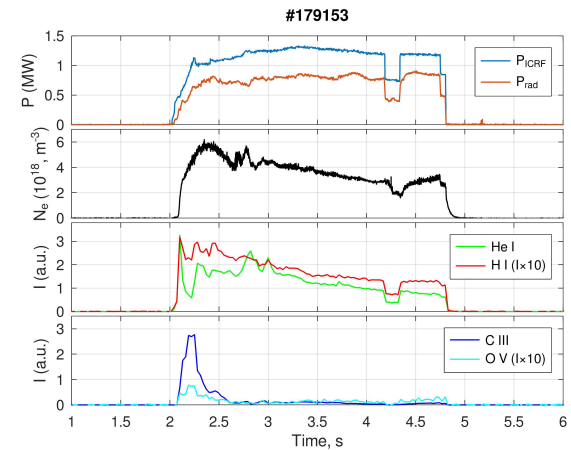


Fig. 5 Time evolutions of injection power  $P_{\text{ICRF}}$  (total), radiation power  $P_{\text{rad}}$ , average electron density  $N_e$ , optical emission intensities of H I ( $\text{H}\alpha$  656.3 nm), He I (587.6 nm), C III (97.7 nm) and O V (63 nm). The working gas content is  $\sim 25\% \text{ H}_2 + 75\% \text{ He}$ .  $B_0 = 2.75 \text{ T}$ .

periments [12]. This is also indicated by the high intensity of spectral lines in the ICRF discharge as compared to the ECRH discharge. The absence of an increase in the spectral line intensity due to recombination after the ICRF discharge should be noticed.

In the regime without pre-ionization the breakdown and production of ICRF plasma with a density is much below  $10^{17} \text{ m}^{-3}$  occurs in a short time of  $\sim 10 \text{ ms}$ . This stage is characterized by the beginning of the growth of the intensity of the spectral lines of the H I and He I atoms (see Fig. 5). The plasma density of  $\approx 1 \times 10^{17} \text{ m}^{-3}$  is reached for a time of  $\sim 60 \text{ ms}$  after the start of the RF pulse. The intensities of the spectral lines of the O V and C III ions begin to increase. The maximum density of  $\approx 6 \times 10^{18} \text{ m}^{-3}$  is reached at RF power of  $\approx 1 \text{ MW}$ . Radiation losses are

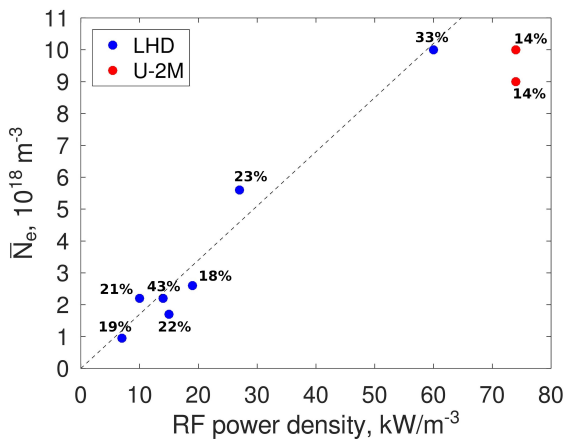


Fig. 6 Dependence of maximum plasma density on RF power density in LHD and U-2M. The percentage values near the dots correspond to the initial concentration of hydrogen in the gas mixture  $H_2+He$ .

≈ 0.75 MW. The subsequent decrease in the intensity of the spectral lines of the O V and C III impurities and the plasma density seems to be related to decrease of the electron temperature. The main features of the ICRF discharge are: breakdown and the beginning of plasma creation occurs in a short time, the formed plasma has a low temperature and is partially ionized, in the plasma there are impurities that leads to high radiation losses.

As the experiments on the LHD show, the plasma density increases as the injected RF power increases. The same dependence was observed in the experiments on U-2M [9, 11]. Figure 6 shows the dependence of maximum plasma density on RF power density. As can be seen from Fig. 6 the plasma density at the level of  $10^{19} m^{-3}$  can be achieved at RF power density at or above  $60 kW/m^3$ . And weakly sensitive to change in the hydrogen concentration in the  $H_2+He$  mixture.

The start-up time covers both the RF breakdown stage and the plasma production stage [9, 31]. Start-up time is different for U-2M and LHD. U-2M has a start-up time less than 20 ms. For LHD this time is in hundreds of milliseconds. The breakdown time in the U-2M is up to a few milliseconds and depends on initial pressure, antenna voltage, magnetic field [9, 16], etc. In U-2M case the plasma density was then increased to a maximum value over during 6 - 10 ms. In the LHD, the breakdown has less fast consuming 10 - 30 ms of time. The density increased over a period of hundreds of milliseconds to a maximum value.

## 5. Summary

The results of the ICRF study of plasma production with hydrogen minority at U-2M and LHD indicate that this scenario can be scaled to large stellarator devices, including W7-X. The scenario can be implemented in relatively weak magnetic fields ~0.3 T as well as in strong ones ~2.7 T. The condition of the presence of the ion cyclotron

resonance zone for the fundamental harmonic of hydrogen inside the plasma column should be fulfilled for this method. Accordingly, it seems possible to implement this scenario in a magnetic field of ~1.7 T for W7-X. The scenario is weakly sensitive to change in the hydrogen concentration in the  $H_2+He$  mixture. And the optimal hydrogen concentration needed to obtain the high density lies in the range ~10 - 20% hydrogen in the  $H_2+He$  mixture. No critical differences were observed in plasma production by the different antenna types. Likely, the ICRF system of W7-X can be used to try this scenario. The achieved plasma density of  $\sim 10^{19} m^{-3}$  is quite suitable as a target plasma for subsequent NBI. However, the achieved electron temperature is low for a successful start of X3-mode ECRH at W7-X. Calculations show that an electron temperature of ~0.7 keV is required [7]. Therefore, the main goal of future experiments will be to find conditions to realize ICRF plasma heating to high temperatures within this scenario.

## Acknowledgment

This work has been carried out within the framework of the EUROfusion Consortium, funded by the European Union via the Euratom Research and Training Programme (Grant Agreement No 101052200 — EUROfusion). Views and opinions expressed are however those of the author(s) only and do not necessarily reflect those of the European Union or the European Commission. Neither the European Union nor the European Commission can be held responsible for them.

- [1] F. Warmer *et al.*, Plasma Phys. Control. Fusion **58**, 074006 (2016).
- [2] V. Erckmann *et al.*, Fusion Sci. Technol. **52**, 291 (2007).
- [3] M. Endler *et al.*, Fusion Eng. Des. **167**, 112381 (2021).
- [4] J. Ongena *et al.*, Phys. Plasmas **21**, 061514 (2014).
- [5] D.A. Castaño Bardawil *et al.*, Fusion Eng. Des. **166**, 112205 (2021).
- [6] A. Lazerson *et al.*, Nucl. Fusion **61** 096008 (2021).
- [7] N.B. Marushchenko *et al.*, EPJ Web Conf. **203**, 01006 (2019).
- [8] V.E. Moiseenko *et al.*, J. Plasma Phys. **86**, 905860517 (2020).
- [9] V.E. Moiseenko *et al.*, J. Fusion Energy **41**, 15 (2022).
- [10] Yu.V. Kovtun *et al.*, Plasma Fusion Res. **17**, 2402034 (2022).
- [11] Yu.V. Kovtun *et al.*, 32nd Symposium on Fusion Technology, 18-23 September 2022, Dubrovnik, Croatia, P-2.322.
- [12] S. Kamio *et al.*, Nucl. Fusion **61**, 114004 (2021).
- [13] V. Bykov *et al.*, Fusion Technol. **17**, 140 (1990).
- [14] O.S. Pavlichenko, Plasma Phys. Control. Fusion **35**, B223 (1993).
- [15] V.E. Moiseenko *et al.*, Nucl. Fusion **51**, 083036 (2011).
- [16] V.E. Moiseenko *et al.*, Probl. At. Sci. Technol. Ser.: Plasma Phys. **1**, 263 (2019).
- [17] A.V. Lozin *et al.*, Probl. At. Sci. Technol. Ser.: Plasma Phys. **6**, 10 (2020).
- [18] A. Iiyoshi *et al.*, Nucl. Fusion **39**, 1245 (1999).
- [19] M. Osakabe *et al.*, Fusion Sci. Technol. **72**, 199 (2017).
- [20] S. Kamio *et al.*, Nucl. Fusion **62**, 016004 (2022).

- [21] T. Mutoh *et al.*, Fusion Sci. Technol. **58**, 504 (2010).
- [22] H. Kasahara *et al.*, 38th EPS Conf. Plasma Physics 27 June-1 July 2011, Strasbourg, France.
- [23] K. Saito *et al.*, Fusion Eng. Des. **96-97**, 583 (2015).
- [24] A.V. Lozin *et al.*, Probl. At. Sci. Technol. Ser.: Plasma Electronics and New Methods of Acceleration **4**, 195 (2021).
- [25] H.G. Esser *et al.*, J. Nucl. Mater. **241**, 861 (1997).
- [26] R. Brakel *et al.*, J. Nucl. Mater. **290**, 1160 (2001).
- [27] A. Lyssoivan *et al.*, J. Nucl. Mater. **337-339**, 456 (2005).
- [28] A. Lyssoivan *et al.*, J. Nucl. Mater. **363-365**, 1358 (2007).
- [29] M.K. Paul *et al.*, AIP Conf. Proc. **1187**, 177 (2009).
- [30] A. Lyssoivan *et al.*, J. Nucl. Mater. **390-391**, 907 (2009).
- [31] A. Lyssoivan *et al.*, Plasma Phys. Control. Fusion **54**, 074014 (2012).